Polarisation dependence of ion acceleration from ultrathin foils

C. Scullion, D. Doria, F. Hanton, D. Gwynne, K. Naughton, S. Kar, M.Zepf, M. Borghesi

Centre for Plasma Physics, School of Mathematics and Physics, Queen's University of Belfast, Belfast BT7 1NN, United Kingdom

L. Romagnani

LULI, 'Ecole Polytechnique, CNRS, CEA, UPMC, Palaiseau, France

A. Sgattoni, A. Macchi

Universita di Bologna, Pisa, Italy

P. McKenna

Department of Physics, University of Strathclyde, SUPA, Glasgow G4 0NG, United Kingdom

D. R. Symes

Central Laser Facility, STFC Rutherford Appleton Laboratory, Chilton, Didcot, OX11 0QX, United Kingdom

Introduction

Focusing high-contrast, intense laser pulses onto ultrathin foils allows access to novel laser-matter interaction regimes of relevance to innovative schemes for ion acceleration [1-4]. The very large radiation pressure of an intense laser pulse (10s of Gbar for $I > 10^{20}$ W/cm^2), when applied to a thin enough foil, is predicted to lead, under appropriate conditions, to Light Sail ion acceleration, where a compressed, neutralised ion layer is efficiently driven forward, provided it stays opaque to radiation [5-13]. If decompression of the ionised foil occurs, the target plasma can become relativistically transparent, and propagation of the laser pulse through the target can lead to regimes of enhanced electron heating and bulk ion acceleration [14]. Particularly for ultrashort pulses, the laser polarisation can play a significant role on the amount of electron heating and in determining which of the two above regimes applies; and circular polarisation is thought to create favourable conditions for achieving stable Radiation Pressure Acceleration [13,15].

Background

Target normal sheath acceleration (TNSA) is the basic mechanism of the acceleration of protons from solid targets. In TNSA, the energetic "fast" electrons accelerated at the front surface, where the laser-plasma interaction occurs, accelerate protons by the sheath field generated at the rear surface of the target. A very intense current of high energy hot electrons generated at the front side of the target eventually reach the rear side, where a cloud of relativistic electrons is formed and extend out of the target for several Debye lengths giving rise to an extremely intense electric field, mostly directed along the normal to the target surface. This large field will hold back most of the escaping electrons, ionise atoms at the rear surface, and start to accelerate ions perpendicularly to the surface. The electric field generated at the rear surface depends on the electron distribution parameters of temperature, number and divergence as well as the density profile. TNSA ion beams typically have a broad energy spectrum, modest conversion efficiency at high energies, large divergence and $E \propto I\lambda^{1/2}$ scaling of maximum proton energy (E) with peak laser intensity (I) [1-4].

Radiation pressure acceleration (RPA) is a less established mechanism with less experimental evidence than TNSA, since TNSA dominates for typical interaction conditions. RPA is classified differently depending on the target thickness; in thicker targets, hole boring occurs, whereas in thin targets where all the ions are accelerated before the end of the laser pulse, the light sail mechanism (LS) takes place. The final energy should simply scale as $\propto (I\tau/\sigma)^\alpha$ (where I is the intensity, τ the pulse duration and σ is the areal mass density of the foil). The exponent α is equal to 2 for v_{final} and

$\alpha \to 1/3$ in the ultrarelativistic limit [10]. In thin targets, the whole laser-irradiated area is detached and pushed forward by the radiation pressure. The laser further accelerates ions to higher energies since the ions are not screened by a background plasma. Among the RPA mechanisms the LS mechanism has many attractive features; there is a high laser ion conversion efficiency and a possibility of reaching very high energies, a favourable dependence on the laser fluence, a natively narrow energy spectrum, a reduced divergence, and a similarly efficient acceleration for both protons and higher mass ions, as predicted by numerous computational and analytical studies [5,6,10,13].

As mentioned above, an important role in the RPA is played by the polarisation of the laser pulse by controlling the electron heating and consequently determining which acceleration mechanism dominates [13]. Circular polarisation (CP) is thought to create favourable conditions for achieving stable RPA compared to linear polarisation (LP) owing to a lesser electron heating, which for ultrathin foils prevents (or delays) the onset of relativistic transparency during laser irradiation.

In this experiment the effect of the laser light polarisation on the acceleration of ions from ultrathin foils was investigated. The ion beam was characterised, inducing information on the quantity, type, energy and distribution of ions produced to determine the optimum configuration for the acceleration process for use in future investigations.

Experimental Setup

The experiment was carried out on the Astra Gemini laser facility at the Rutherford Appleton Laboratory, employing 40 fs laser pulses with controllable polarisation, focused at normal incidence onto a carbon foil by an *f*/2 parabolic mirror up to intensities of ~ 3×10^{20} W/cm^2.
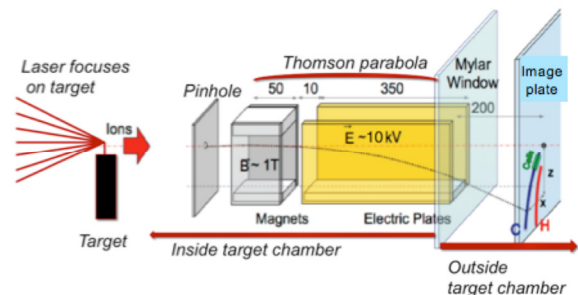
Figure 1. A sketch of the experimental setup.

The laser light polarisation (circular or linear) was controlled by a quarter waveplate. A double plasma mirror configuration was employed to improve the temporal contrast of the laser beam allowing a suitable interaction with ultrathin targets. Three
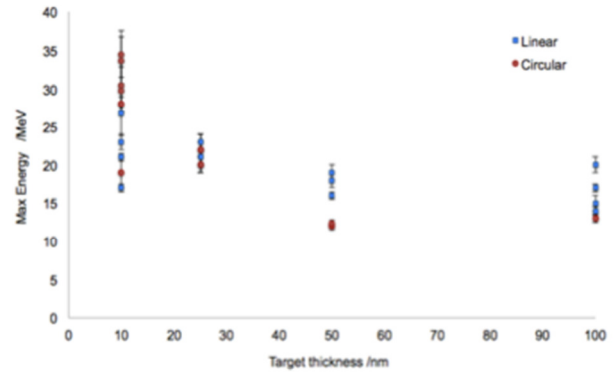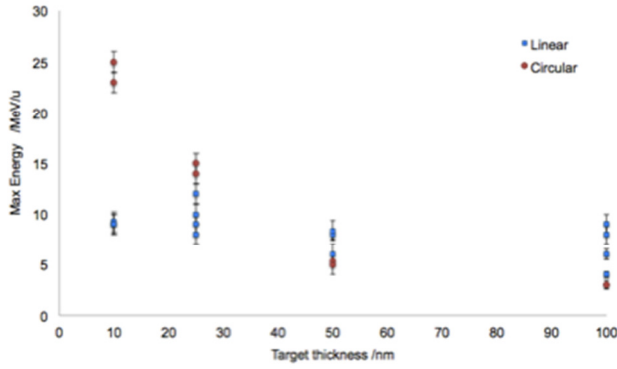
Figure 2. Maximum energy of carbon ions (left) and protons (right) for linearly (blue) and circularly (red) polarised laser light as a function of target thickness.

different types of detector were employed to gather information on the characteristics of the ions: a Thomson parabola (TP) spectrometer with an image plate as detector, radiochromic film (RCF) and CR-39 stacks.

Results

We have observed a strong dependence of the characteristics of accelerated ions from the target thickness and the laser polarisation. The highest proton and carbon energies (up to 25-30 MeV/nucleon) were observed for circularly polarised pulses and 10 nm targets. A strong difference in the beam profile is observed for linearly and circularly polarised pulses. The main characteristics of the data are reproduced by 3D Particle in Cell simulations. Figure 3 shows RCF for linearly and circularly polarised laser pulses for both experimental data and simulations.
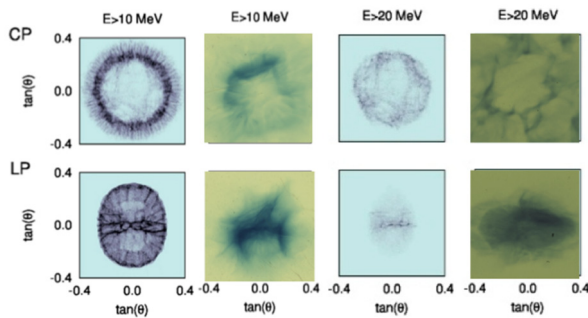
Figure 3. Simulation (blue) and experimental (green) RCF beam profiles for circular polarization (top) and linear polarisation (bottom) for proton energies greater than 10 MeV (left) and 20 MeV (right).

The maximum energy of protons (left) and carbon ions (right) for varying target thicknesses were deduced from TP spectra and from RCF stacks. It can be seen that for thinner targets
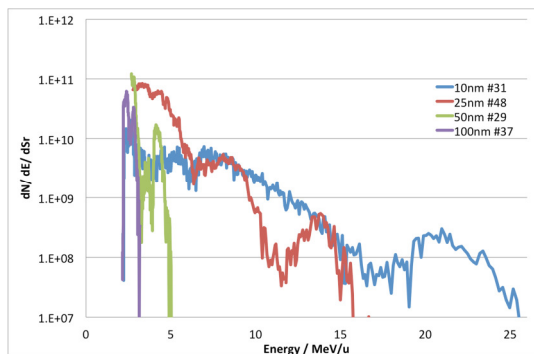
Figure 4. Thomson parabola spectra for carbon ions for targets of various thicknesses irradiated by circularly polarised laser pulses.

circularly polarised laser pulses give rise to higher energy protons and carbon ions. The spectra for carbon ions created by circularly polarised laser pulses are shown in Figure 4. It can be seen that the maximum energy of carbon ions is obtained for 10nm targets. These were the thinnest targets used.

Conclusion

These results provide possible evidence of a regime in which RPA is the dominant acceleration mechanism since hot electron heating is reduced. The maximum energy of Carbon ions and protons is obtained for targets of thickness 10nm (thinnest targets used) for circularly polarised laser pulses. This is the first time that circularly polarised laser pulses have produced ions of higher energies than linearly polarised pulses under the same interaction conditions.

References

1. M. Borghesi, J. Fuchs, S. V. Bulanov, A. J. MacKinnon, P.K. Patel, and M. Roth, Fusion Sci. Technol. 49, 412 (2006);
2. H. Daido, M. Nishiuchi, and A. S Pirozhkov, Rep. Prog. Phys. 75, 056401 (2012);
3. J. Fuchs et al., Nat. Phys. 2, 48 (2006);
4. M. Passoni, L. Bertagna, and A. Zani, New J. Phys. 12, 045012 (2010).
5. A. Macchi, S. Veghini, and F. Pegoraro, Phys. Rev. Lett. 103, 085003 (2009).
6. A. Macchi, S. Veghini, T. V. Liseykina, and F. Pegoraro, New J. Phys. 12, 045013 (2010).
7. B. Qiao, M. Zepf, M. Borghesi, and M. Geissler, Phys. Rev. Lett. 102, 145002 (2009).
8. B. Qiao, M. Zepf, M. Borghesi, B. Dromey, M. Geissler, A. Karmakar, and P. Gibbon, Phys. Rev. Lett. 105, 155002 (2010).
9. B. Qiao, M. Zepf, P. Gibbon, M. Borghesi, B. Dromey, S. Kar, J. Schreiber, and M. Geissler, Phys. Plasmas 18, 043102 (2011).
10. A. P. L. Robinson, M. Zepf, S. Kar, R. G. Evans, and C. Bellei, New J. Phys. 10, 013021 (2008).
11. O. Klimo, J. Psikal, J. Limpouch, and V. T. Tikhonchuk, Phys. Rev. ST Accel. Beams 11, 031301 (2008).
12. X.Q. Yan, C. Lin, Z. Sheng, Z. Guo, B. Liu, Y. Lu, J. Fang, and J. Chen, Phys. Rev. Lett. 100, 135003 (2008).
13. A. Henig et al., Phys. Rev. Lett. 103, 245003 (2009).
14. L. Yin, B. J. Albright, B. M. Hegelich, and J. C. Ferna'ndez, Laser Part. Beams 24, 291 (2006).
15. S. Kar et al., Phys. Rev. Lett. 109, 185006 (2012).